Available online at www.sciencedirect.com

SCIENCE DIRECT

Developmental Biology 295 (2006) 678–688

DEVELOPMENTAL BIOLOGY

www.elsevier.com/locate/ydbio

Identification and lineage tracing of two populations of somatic gonadal precursors in medaka embryos

Shuhei Nakamura [a,b], Daisuke Kobayashi [c], Yumiko Aoki [a,b], Hayato Yokoi [d], Youko Ebe [b], Joachim Wittbrodt [e], Minoru Tanaka [a,*]

[a] *Laboratory of Molecular Genetics for Reproduction, National Institute for Basic Biology, Higashiyama, Myodaiji, Okazaki 444-8787, Japan*
[b] *Division of Biological Sciences, Graduate School of Science, Hokkaido University, Kita-ku, Kita 10, Nishi 8, Sapporo 060-0810, Japan*
[c] *Department of Biological Sciences, Graduate School of Science, University of Tokyo, 7-3-1 Hongo, Bunkyo-ku, Tokyo 113-0033, Japan*
[d] *Institute of Neuroscience, University of Oregon, Eugene, OR 97403, USA*
[e] *Developmental Biology Programme, EMBL, Meyerhofstrasse 1, 69012 Heidelberg, Germany*

Received for publication 7 October 2005; revised 30 March 2006; accepted 31 March 2006
Available online 7 April 2006

Abstract

The gonad contains two major cell lineages, germline and somatic cells. Little is known, however, about the somatic gonadal cell lineage in vertebrates. Using fate mapping studies and ablation experiments in medaka fish (*Oryzias latipes*), we determined that somatic gonadal precursors arise from the most posterior part of the *sdf-1a* expression domain in the lateral plate mesoderm at the early segmentation stage; this region has the properties of a gonadal field. Somatic gonadal precursors in this field, which continuously express *sdf-1a*, move anteriorly and medially to the prospective gonadal area by convergent movement. By the stage at which these somatic gonadal precursors have become located adjacent to the embryonic body, the precursors no longer replace the surrounding lateral plate mesoderm, becoming spatially organized into two distinct populations. We further show that, prior to reaching the prospective gonadal area, these populations can be distinguished by expression of either *ftz-f1* or *sox9b*. These results clearly indicate that different populations of gonadal precursors are present before the formation of a single gonadal primordium, shedding new light on the developmental processes of somatic gonadal cell and subsequent sex differentiation.

Keywords: Gonad; Precursors; *sdf-1a*; *ftz-f1*; *amh*; *sox9b*; Field; Lateral plate mesoderm; Medaka; Fate mapping

Introduction

Organs are formed from cells in a developmental field, classically defined as a region containing precursor cells for that organ (Huxley and De Beer, 1934; DeRobertis et al., 1991). While fate mapping studies of organs, such as the heart, kidney, and blood islands, have identified organ precursor cells that commit to particular lineages during the course of embryonic development (Drummond, 2002; Thisse and Zon, 2002), little is known of gonadal precursors.

The gonad is formed by the coordinated development of two very different cell lineages: germ cells and the somatic gonadal mesoderm that surrounds the germ cells. Although both cell lineages are important for gonadal development, the origin and development of these vertebrate somatic gonadal precursors remain largely unexplored. The development of germ cells and their incorporation into the gonad have previously been described in the teleost fish medaka (*Oryzias latipes*) (Hamaguchi, 1982; Shinomiya et al., 2000; Tanaka et al., 2001; Kurokawa et al., 2006). Primordial germ cells (PGCs) are first recognized at the early gastrula stage with the expression of medaka *nanos*, the orthologue of the *Drosophila nanos* gene. After PGCs align bilaterally along the trunk, they migrate posteriorly to form two condensed domains in the ventrolateral region of the developing hindgut. PGCs come in contact with a subpopulation of lateral plate mesodermal cells. The PGCs and lateral plate mesoderm move together to the prospective gonadal region at the dorsal region of the hindgut, where they combine to form a single gonadal primordium. Organogenesis

* Corresponding author. Fax: +81 564 59 5851.
E-mail address: mtanaka@nibb.ac.jp (M. Tanaka).

0012-1606/$ - see front matter © 2006 Elsevier Inc. All rights reserved.
doi:10.1016/j.ydbio.2006.03.052

of the gonad is then initiated, resulting in the formation of bilateral split gonads (Hamaguchi, 1982; Kanamori et al., 1985).

In mammals, the precursors of the adrenal glands and gonads develop from a common primordium, found near the dorsal side of the coelomic epithelium in the region of developing mesonephric tissue. These precursors are marked by expression of Ad4BP/SF1 (Hatano et al., 1996). Cells derived from the region of mesonephric tissue are also important for development of the testis (Martineau et al., 1997; Capel et al., 1999; Tilmann and Capel, 1999). In birds, cells mobilized from mesonephric tissue also contribute to the stromal cells of the gonad (Rodemer et al., 1986). The histological complexity of the mammalian and avian gonadal region makes it challenging to analyze somatic gonad precursor cell differentiation into two major cell types, which in the testis are the Leydig and Sertoli cells and in the ovaries are the theca and granulosa cells. To understand both the formation of the gonads and the subsequent sex differentiation process, it is important to know the processes underlying the development of these cells. The origin and characterization of gonadal precursor(s), however, have largely remained undetermined.

In contrast to the ambiguities and complexities of the developing gonad in mammals and birds, the histological structures present during the formation of the gonadal primordium are relatively simple in medaka fish. In place of the mesonephric tissues seen dorsal to the developing gonad in mammals and birds, two functionally equivalent organs, the pronephros and interrenal organ, form in the anterior region of the medaka trunk, distant from the prospective gonadal region (Oguri, 1961; Morinaga et al., 2004). There are two nephric ducts running from anterior to posterior along the dorsal aorta and few mesenchymal cells around the developing gonadal primordium in medaka (Hamaguchi, 1982; Kanamori et al., 1985). Thus, medaka gonad forms basically without a significant contribution from mesonephros-equivalent tissue. Given its simplicity, the organogenesis of the medaka gonad may represent an evolutionary prototype for that of the vertebrate gonad, providing a model in which to analyze the cellular interactions essential for gonad development and sexual differentiation.

In vertebrates, SDF-1, a chemokine ligand, provides PGCs with directional cues as they migrate towards the gonad (Doitsidou et al., 2002; Ara et al., 2003; Knaut et al., 2003; Molyneaux et al., 2003; Stebler et al., 2004; Kurokawa et al., 2006). Here, we show evidence that precursors of the medaka somatic gonadal mesoderm originate from the posterior-most region of the *sdf-1a* expression domain to which PGCs are attracted. In addition, by the 6 somite stage (stage 21), this region has acquired the characteristics of the gonadal field. We furthermore show that the precursors are spatially organized into two populations and, before the gonadal primordium forms, can be distinguished by different expression of somatic gonadal mesoderm markers, *ftz-f1*, the medaka homologue of mammalian *Ad4BP/SF1* (Luo et al., 1994; Sadovsky et al., 1995), and *sox9b*, a gene essential for testis formation in mammals (Cameron et al., 1996; Kent et al., 1996; Morais da Silva et al., 1996; Bishop et al., 2000). These results clearly demonstrate that separate populations of somatic gonadal precursors that arise from the gonadal field are established before they initiate gonadal organogenesis, including sex differentiation.

Material and methods

Fish and developmental stages

The medaka (*O. latipes*) inbred strain cab was used for all experiments. Developmental stages of embryos were determined using developmental staging tables (Iwamatsu, 1994; Iwamatsu, 2004).

cDNA cloning of medaka sdf-1a, amh, and sox9b homologues

A 263-bp fragment of medaka *sdf-1a* was isolated by PCR using degenerate PCR primers designed by alignment with vertebrate *SDF-1* genes [forward: 5′-CATGGAYVYCAARGTBVT-3′, and reverse: 5′-TTGTTBADRGCKTTSTY-CAGGTACT-3′ (1st PCR) or 5′-GCKTTSTYCAGGTACTSYTGRGAKCCA-3′ (2nd PCR)]. A full-length sequence of *sdf-1a* was obtained by 5′ RACE and 3′ RACE using FirstChoice RLM-RACE (Ambion) using PCR primers [5′ RACE: 5′-CAGCCACACGCCCACG-3′ (1st PCR) and 5′-ATCACCCTGCTCGC-CAGC-3′ (2nd PCR), 3′ RACE: 5′-GAGCTCAAGTTCCTCCACA-3′ (1st PCR) and 5′-ACGCCCAACTGCCCCTTCCA-3′ (2nd PCR)]. Cloned fragments were identified by sequencing and comparison to known vertebrate *SDF-1* homologues. Phylogenetic and syntenic analysis indicated that our clone (Genbank Accession Number AB214908), which differed from a previously reported medaka *sdf-1* clone (*mfsdf1*) (Yasuoka et al., 2004), is involved in PGC migration (Kurokawa et al., 2006). Therefore, we designated our clone medaka *sdf-1a*.

A 111-bp fragment of medaka *amh* was isolated by RT-PCR with degenerate PCR primers specific for *amh* (forward: 5′-AGAGAATTCCCNTGYT-GYGTNCC-3′ and reverse: 5′-GTGCTCGAGNCKRCANCCRCAYTC-3′). Based on this sequence data, we identified from a medaka testicular library a 4.5-kb clone (NCBI accession number: AB214971) identical to the clone from NCBI accession number AY899284.

A 600-bp medaka *sox9b* fragment was amplified from the medaka genome with degenerate PCR primers (forward: 5′-CCSAGYMTKTCYGAK-GACTCCGC-3′ and reverse: 5′-CT GCTCAGCTCRCCRATRCCAC-3′). The *sox9b* clone that we identified was identical to the clone from NCBI accession number AY870393 (Kluver et al., 2005).

Construction of chimeric RNA to visualize the germ cells in vivo

A medaka *nanos* cDNA clone was obtained from the medaka EST database (NCBI accession number BJ529089). A 132-bp *nanos* 3′ UTR fragment was subcloned into the *Not*I/*Nsi*I site of pRCS21, which encodes the DsRed2 gene (Clontech), to synthesize chimeric RNA (Kurokawa et al., 2006). Capped chimeric RNA of DsRed *nos* 3′ UTR RNA for microinjection was transcribed from the linearized plasmid using an SP6 mMESSAGE mMACHINE Kit (Ambion).

In situ hybridization, immunohistochemistry, and histology

Whole mount in situ hybridization was performed as previously described (Oliver et al., 1996). Antisense DIG-labeled RNA probes for *ftz-f1* [(Watanabe et al., 1999), NCBI accession number AB016834], *amh*, *sdf-1a*, *sox9b*, *wt1* (NCBI accession number AB070576), *lim1* (NCBI accession number AB071189), and *gata2* (NCBI accession number AB183298) were prepared using a DIG labeling kit (Roche). When detecting both RNA expression and OLVAS protein in the same sample, in situ hybridization was performed first. Endogenous OLVAS protein was detected subsequently using polyclonal rabbit anti-OLVAS serum (1:100 dilution) followed by a secondary goat anti-rabbit antibody coupled to Alexa 488 or Alexa 568 (Molecular Probes). Stained embryos were counter-stained with 1% neutral red or toluidine blue, embedded in Jung HistoResin Plus (Leica), sectioned (1 or 3 μm), and mounted in Eukitt.

Cell labeling using caged fluorescein

Cell tracing experiments using caged fluorescein were performed as previously described (Serluca and Fishman, 2001). We injected a 2.5% solution of DMNB-caged fluorescein dextran (Molecular Probes) and 5 mg/ml phenol red in 0.2 M KCl into medaka embryos at the 1- to 2-cell stage. Injected embryos were maintained at 29°C until the designated stage. At the 6 somite (stage 21) and 10 to 11 somite (stages 22–23) stages, embryos were placed in a 1.5% agarose mold. Uncaging was performed by nitrogen laser pulsing at 375 nm (MicroPoint Laser System, Photonic Instruments) and focused by a 40× (Olympus) or 63× (Zeiss) water-immersion objective on a Zeiss Axioscop 2 plus microscope. DIC and fluorescence images were acquired using a cooled CCD camera (Hamamatsu Photonics) equipped with shutters controlled by Aquacosmos (Hamamatsu Photonics). A subset of the labeled embryos were fixed immediately, while others were allowed to develop in the dark until the 13 somite stage (stage 23), stage 26, stage 30, or stage 35. Specimens were then fixed in 4% PFA (paraformaldehyde) in PBS. Fixed embryos were incubated with a 1:500 dilution of anti-fluorescein POD (Roche) then incubated in 0.025% 3,3′-diaminobenzidine (SIGMA) solution for chromogenic reaction. To visualize uncaged FITC by fluorescence, we combined tyramide signal amplification (TSA Biotin System; Perkin Elmer) with immunohistochemistry according to the manufacturer's instructions. The resulting biotin precipitates were visualized with a 1:100 dilution of streptavidin Alexa 488 (Molecular Probe). Sections were counterstained with Hoechst 33342 (Molecular Probe) to visualize the nucleus.

Cell ablation

Cell ablation studies were performed as described previously (Serbedzija et al., 1998). Embryos were mounted and positioned in agarose molds at the 6 somite stage (stage 21), 10 somite stage (stage 22–23), 14 somite stage (stage 24), stage 26, and stage 28. The laser, set at 440 nm, was focused on the lateral mesoderm cells. Cell death was confirmed by either staining with To-pro 1 (Molecular Probe) or the absence of *sdf-1a* expression by in situ hybridization. Embryos were maintained at 29°C until reaching stage 35. Embryos were then fixed in 4% PFA and subjected to in situ hybridization for either *ftz-f1* or *amh* followed by immunohistochemistry with the combination of an anti-medaka OLVAS antibody and an Alexa-488-conjugated goat anti-rabbit IgG secondary antibody (Molecular Probe). At stage 28, a certain population of somatic gonadal precursors surround PGCs. Therefore, we performed laser ablation of somatic gonadal precursors, including some PGCs.

Results

Expression of ftz-f1 defines mesodermally derived gonadal precursors

In mammals, the primordia of both the adrenal glands and gonads are derived from *Ad4BP/SF1*-expressing somatic cells (Hatano et al., 1996). Disruption of this gene impairs the development of both organs (Luo et al., 1994; Sadovsky et al., 1995), indicating that *Ad4BP/SF1* is essential for the establishment of somatic gonadal mesoderm. To analyze the development of the medaka somatic gonadal mesoderm during embryogenesis, we examined the expression of *ftz-f1* (Watanabe et al., 1999), the medaka *Ad4BP/SF1* orthologue. At stage 33, *ftz-f1* is expressed in the somatic gonadal mesoderm (blue staining in Figs. 1C and D). *ftz-f1*-positive cells surrounded the germ cells (green fluorescence) in the gonadal primordium located dorsal to the developing hindgut and ventral to the nephric ducts at the levels of eleventh and thirteenth somites anterior–posteriorly. Unexpectedly, expression of *ftz-f1* was detected as early as stage 30 in a subpopulation of lateral plate mesoderm intervening primordial germ cells (PGCs) with thin cytoplasmic processes (Fig. 1A). Although expression of *ftz-f1* was detected as punctate spots on thin sections (Fig. 1B), the results were reproducible at stage 30. Punctate expression was sometimes seen by in situ hybridization when the transcripts

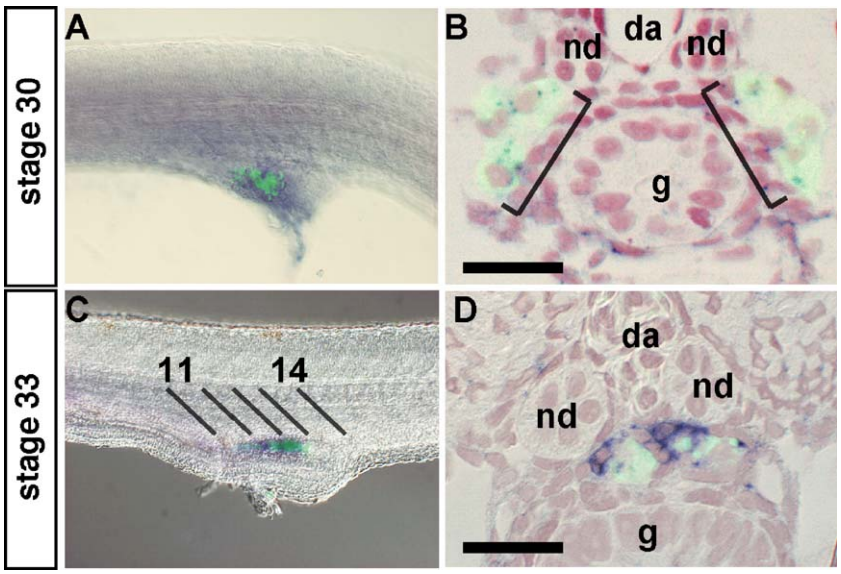

Fig. 1. Gonadal somatic mesoderm is established before formation of the gonadal primordium. Double staining of the gonadal mesoderm marker *ftz-f1* (purple) and the germline marker OLVAS (green fluorescence). All images are bright field images with the fluorescent images overlaid. (A and C) Lateral views. Anterior is on the left. (B and D) Transverse sections were counterstained with neutral red. (A and B) Stage 30: PGCs are located lateral to the hindgut. *ftz-f1* expression was first found in a subpopulation of the lateral mesoderm surrounding the PGCs. (B) Punctate expression of *ftz-f1* lateral to the developing hindgut is indicated by brackets. (C and D) Stage 33: PGCs are found in the gonadal primordium, ventral to the nephric ducts and dorsal to the hindgut. *ftz-f1* expression is observed in the somatic gonadal mesoderm at the levels of the eleventh to thirteenth somites. The black lines denote the somite boundaries. (da), dorsal aorta. (nd), nephric duct. (g), hindgut. Scale bar, 20 μm.

localized to small areas of the cytoplasm (Kosman et al., 2004; Ronshaugen and Levine, 2004). This expression pattern likely represents somatic gonadal precursor cells located in the posterior lateral plate mesoderm; it is unlikely to mark the interrenal (adrenal gland-equivalent organ) primordium as *ftz-f1*-positive interrenal progenitors are located in a more anterior region, close to the developing pronephros (Oguri, 1961; Morinaga et al., 2004). These data indicate that the somatic gonadal mesoderm is established by stage 30 at bilateral positions to the developing hindgut, suggesting that *ftz-f1*-expressing mesodermal cells move dorsally with PGCs to the prospective gonadal region, where a single gonadal primordium forms and initiates organogenesis including the process of sex differentiation.

sdf-1a expression becomes restricted to the posterior lateral plate mesoderm

Next, we examined the origin of gonadal mesodermal cells expressing *ftz-f1* and surrounding PGCs at stage 30. As the PGCs are guided by SDF-1a towards the prospective gonadal region in zebrafish, chickens, and mice (Doitsidou et al., 2002; Ara et al., 2003; Knaut et al., 2003; Molyneaux et al., 2003; Stebler et al., 2004; Kurokawa et al., 2006), we hypothesized that somatic gonadal precursors originated from *sdf-1a*-expressing cells.

We first investigated the patterns of *sdf-1a* expression. At the 6 somite stage (stage 21), *sdf-1a* is broadly expressed throughout the lateral plate mesoderm (Fig. 2A). As somitogenesis proceeds, *sdf-1a* expression becomes restricted to the posterior and medial portions of the lateral plate mesoderm (blue staining in Figs. 2B–D). At this point, PGCs were clustered around the anterior boundary of the *sdf-1a* expression domain (Fig. 2D). At stage 30, *sdf-1a* was expressed in mesodermal cells covering the developing hindgut, which included both cells surrounding the PGCs lateral to the hindgut and those located more dorsally beneath the nephric ducts (Fig. 2E). By the time PGCs reached the prospective gonadal region at stage 33, *sdf-1a* expression was downregulated in somatic cells (data not shown).

Somatic gonadal precursors occupy the posterior-most region of the sdf-1a expression domain

To map the positions of somatic gonadal precursors, we labeled a group of five to ten cells inside and outside of the *sdf-1a* expression domain using caged fluorescein (Fig. 3, Supplementary Fig. 2, Table 1). After marking the cells by

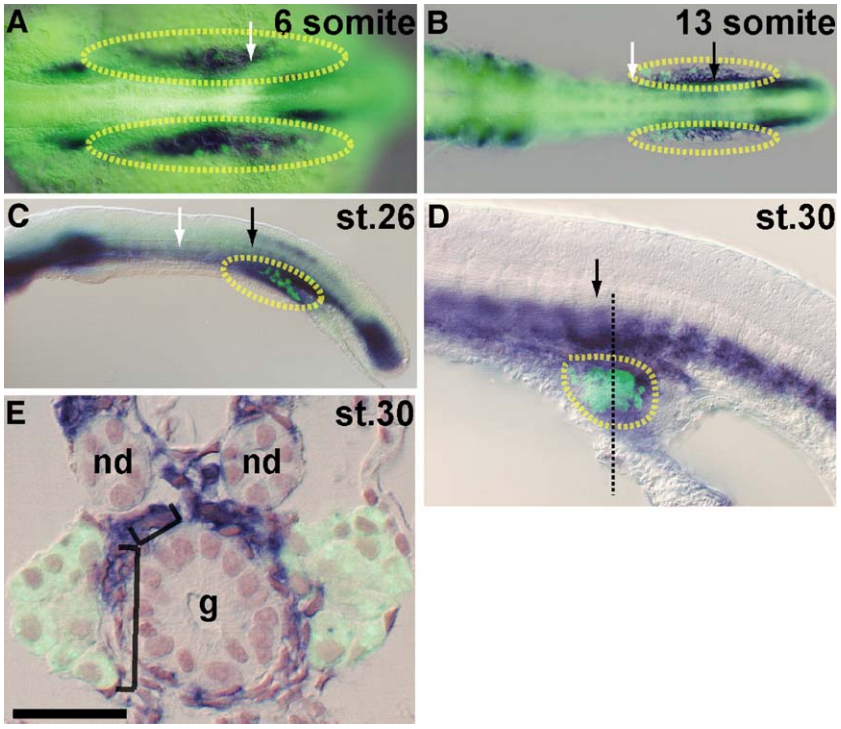

Fig. 2. *sdf-1a* and OLVAS expression. (A–E) Double staining of *sdf-1a* (purple) and the germline marker OLVAS (green fluorescence). The yellow dotted circles indicate the *sdf-1a* expression domains in the lateral plate mesoderm. Fluorescent images are overlaid on the bright field images. White arrows indicate the position of the sixth somite, while black arrows indicate the eleventh somite. (A and B) Dorsal views. (C and D) Lateral views. (A) 6 somite stage (stage 21): *sdf-1a* transcripts were detected broadly throughout the lateral mesoderm, while PGCs were scattered throughout the lateral plate mesoderm. (B) 13 somite stage (stage 23): *sdf-1a* expression in the lateral mesoderm was posteriorly and medially restricted, while PGCs were bilaterally aligned in the anterior *sdf-1a* expression domain. (C) Stage 26: *sdf-1a* expression in the lateral plate mesoderm was restricted posteriorly and medially, while the PGCs migrated posteriorly to the *sdf-1a* expression domain. (D) Lateral view of a stage 30 embryo. (E) A cross-section taken where indicated at the level of the black line in D. *sdf-1a* expression in the lateral plate mesoderm was seen both in the region lateral to the hindgut around the PGCs and in the medially located region beneath the nephric ducts (shown by different brackets). (nd), nephric duct. (g), hindgut. Scale bar, 20 μm.

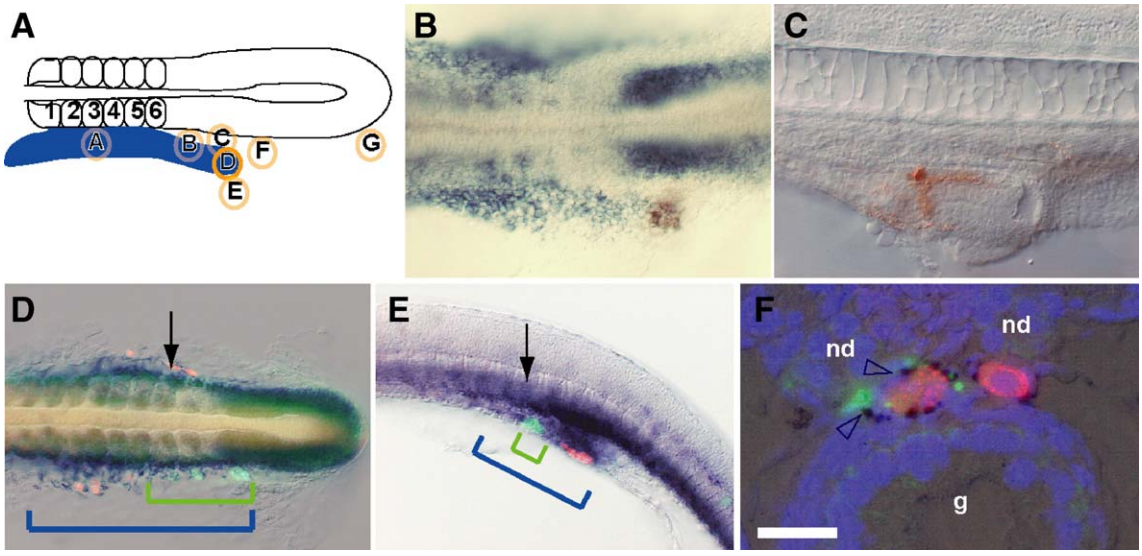

Fig. 3. Cells in the posterior of the *sdf-1a* expression domain contribute to the somatic gonadal mesoderm. (A) The schematic diagram indicates the locations of uncaged cells with respect to the *sdf-1a* expression domain (blue) in the lateral plate mesoderm at the 6 somite stage (stage 21). The cells in region D just after uncaging (B) and their descendants at stage 35 (C) were visualized by antibody staining for uncaged fluorescein (brown). (D, E, and F) The progeny of the region D uncaged cells was visualized at later developmental stages [D: 13 somite stage (stage 23), E: stage 26, and F: stage 35] by antibody staining for uncaged fluorescein (green fluorescence indicated by green brackets). The black arrows indicate the position of the eleventh somite. Expression of *sdf-1a* (blue staining in panels D and E) in the lateral plate mesoderm is indicated by blue brackets. *ftz-f1* expression (dark blue staining in panel f) within the gonad is indicated by dark blue arrowheads. PGCs are labeled by red fluorescence. Sections were counterstained with blue fluorescence of Hoechst 33342 (f). (nd), nephric duct. (g), hindgut. Scale bar, 20 μm.

uncaging at the 6 somite stage (stage 21, Fig. 3A), the location of the marked progenitor cells was determined by whole mount antibody staining (Figs. 3B to F). We determined that labeled cells from the posterior-most region of the *sdf-1a* expression domain only (region D, Figs. 3A and B) were later positioned in the gonadal region (between the eleventh and thirteenth somites) at stage 35 (Fig. 3C, $n = 21$). We next investigated how the labeled cells moved to reach the gonadal area by examining their relative position to PGCs and the *sdf-1a* expression domain. At the 13 somite stage (stage 23), cells that had been labeled in region D were identified posterior to the level of the eleventh somite (green fluorescence in Fig. 3D) in the posterior-most part of the *sdf-1a* expression domain (blue staining). Many PGCs (red fluorescence) were located anterior to the labeled cells. The labeled cells subsequently converged with the *sdf-1a* expression domain medially, although their relative position along the anterior–posterior axis remained unchanged. PGCs began to contact the labeled cells at this stage, stage 26 (Fig. 3E). Finally, the labeled cells (green fluorescence) gave rise to cells surrounding the germ cells (red fluorescence) in the gonadal region by stage 35 (Fig. 3F). In situ analysis indicates that the labeled cells express *ftz-f1* near PGCs in the gonad (arrowheads in Fig. 3F).

We further confirmed that the posterior-most region of the lateral plate mesoderm moved anteriorly and medially by convergent extension movement (Keller et al., 2000) and met PGCs to form the gonadal primordium (Supplementary Fig. 1). Somatic cells were visualized by a photoactivatable GFP variant (PA-Venus) (Nagai et al., 2002; Patterson and Lippincott-Schwartz, 2002;) in medaka bearing fluorescent PGCs (Kurokawa et al., 2006). The in vivo imaging results also support our conclusion that the posterior lateral plate mesoderm, which was marked by PA-Venus, moved anteriorly and medially to locate in close proximity to posteriorly migrating PGCs. In contrast,

Table 1
Tracing the fate of cells inside or outside the *sdf-1* expression domain

Uncaged region (see diagram in Fig. 3A)	Anterior–posterior position of labeled cells at stage 35 relative to somite level				Total no. of uncaged embryos
	1st–3rd somite	4th–10th somite	11th–13th somite	14th somite <	
A	21				21
B		16			16
C			2 (gonad), 7 (dorsal aorta)	2	11
D			21 (gonad)		21
E			10 (skin)		10
F			1 (ventral to gut)	11	11
G				9	9

Uncaging was performed inside or outside of the *sdf-1* expression domain at the 6 somite stage, and embryos were allowed to develop until stage 35. The lineage tracer was visualized by antibody staining. The 11th–13th somite level corresponds to the location of the gonadal primordium.

Table 2
Ablation of somatic gonadal precursors at various developmental stages

Stage of ablation of the gonadal field	No. of embryos with reduced *ftz-f1* expression at stage 35	Total *n*	No. of embryos with reduced *amh* expression at stage 35	Total *n*
Stage 21 (6 somites)	0	15	0	11
Stages 22–23 (10–11 somites)	0	10	0	14
Stage 24 (14 somites)	3	13	1	11
Stage 26	9	10	6	9
Stage 28	11	12	8	11

After bilateral ablation of the somatic gonadal precursors at various developmental stages, embryos were allowed to develop until stage 35 in order to examine the gene expression of gonadal markers, *ftz-f1* and *amh*.

cells outside of region D did not contribute to the gonadal region at stage 35 (Table 1, Supplementary Fig. 2). Our analyses identified the posterior part of the *sdf-1a* expression domain at 6 somite stage as the region in which somatic gonadal precursors arise.

The somatic gonadal precursors are not replaceable after stage 26

To examine the time at which the somatic gonadal mesoderm became committed to this lineage, we performed laser ablation experiments. The posterior-most regions of the *sdf-1a* expression domain were ablated bilaterally using a laser at several different stages. After allowing the ablated samples to develop until stage 35, we examined the expression of the somatic gonadal mesoderm markers *ftz-f1* and *amh* (Münsterberg and Lovell-Badge, 1991) (Table 2). When somatic gonadal precursors were ablated at the 6 somite stage (stage 21), expression of *ftz-f1* and *amh* within the gonadal region was unaffected at stage 35, appearing similar to the unablated controls (Figs. 4A and B, and Supplementary Fig. 3). When ablation was performed at stage 26, however, expression of *ftz-f1* and *amh* was dramatically reduced, despite the presence of somatic cells in the gonadal region at stage 35 (Figs. 4C and D). Thus, the somatic gonadal mesoderm cannot be replaced by other cells following loss of the precursor cells at stage 26 (Table 2).

The posterior-most region of sdf-1a expression at the 6 somite stage (stage 21) has the properties of a gonadal field

To characterize the posterior-most ends of the *sdf-1a* expression domain and to determine the identity of the cells able to replace somatic gonadal precursors ablated at the 6 somite stage (stage 21), we removed the gonadal precursors at the posterior-most end of the *sdf-1a* expression domain on one side of the embryo by laser ablation (Fig. 5C, diagrammed in Figs. 5A and B); we then monitored the movement of adjacent cells that normally do not contribute to the gonad. Six hours after ablation, *sdf-1a* expression reappeared on the ablated side

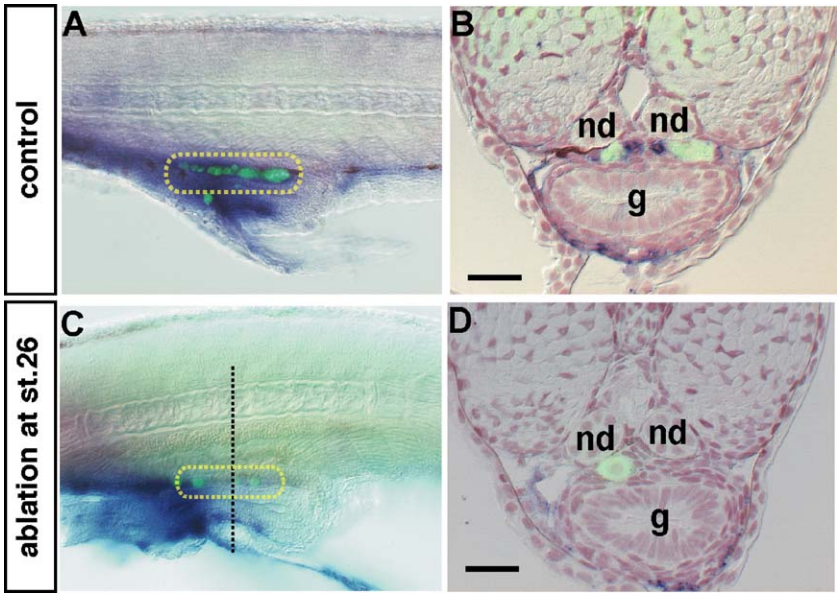

Fig. 4. Ablation of somatic gonadal precursors at stage 26 impairs *amh* expression. (A) OLVAS (green fluorescence) and *amh* expression (purple) in a wild-type embryo at stage 35. (B) A cross-section taken at stage 35 demonstrated that *amh* (purple) is expressed in the cells near the germ cells. Germ cells are labeled in green fluorescence. (C) A stage 35 embryo, in which gonadal precursors were ablated on both sides at stage 26, exhibited reduced *amh* expression (blue staining). (D) Cross-section taken at the levels of the black dotted line in panel C. (A and C) Lateral views. The yellow dotted circles indicate the gonadal area. (nd), nephric duct. (g), hindgut. Scale bar, 20 μm.

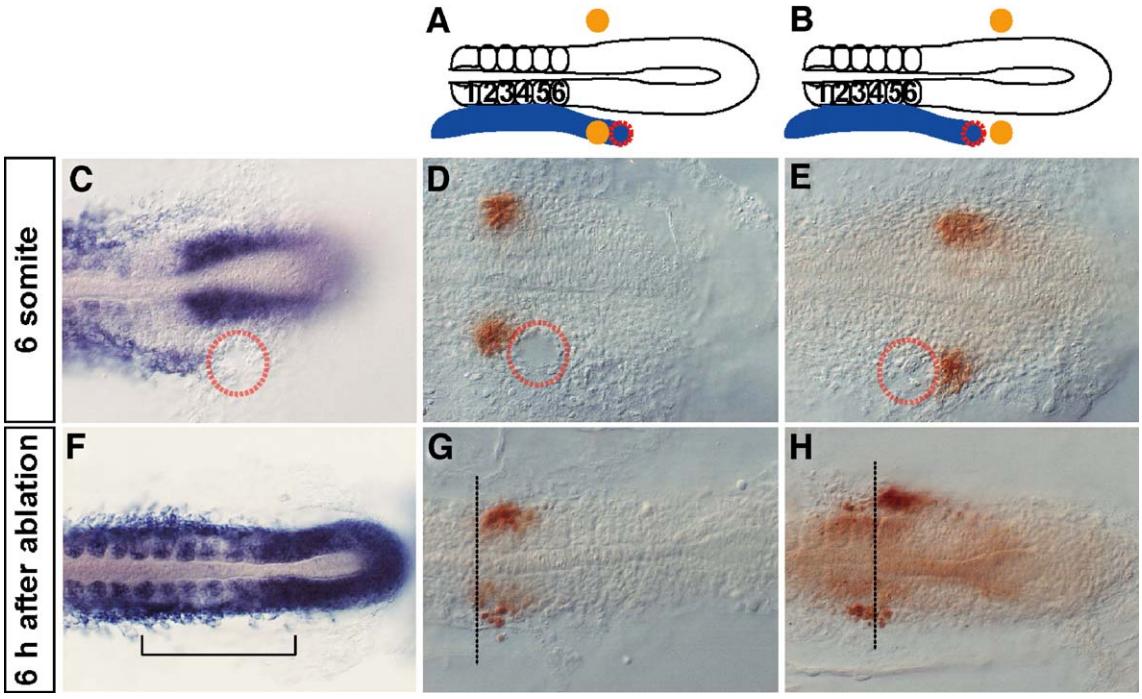

Fig. 5. The most posterior portion of the *sdf-1a* expression domain in the lateral plate mesoderm exhibits the properties of a gonadal field at the 6 somite stage (stage 21). (A and B) The schematic diagrams indicate the locations of the ablated regions, the somatic gonadal precursors (red dotted circles), and the adjacent marked cell by uncaging (brown solid circles). *sdf-1a* expression is indicated in solid blue. (C–E, dorsal views) Six somite stage (stage 21) embryos immediately after ablation. The ablated regions at the posterior end of the *sdf-1a* expression domain are enclosed by red dotted circles. The cells marked by uncaging were visualized with anti-fluorescein staining (brown). (F–H, dorsal views) Embryos 6 h after ablation [13 somite stage (stage 23)]. (C and F) Expression of *sdf-1a* on the ablated side began to recover 6 h after ablation. *sdf-1a* expression in the lateral region is indicated by a bracket. (E and H) Cells posterior to the ablated region migrated more anteriorly to the region where ablated gonadal precursors would otherwise be occupied. (D and G) In contrast, uncaged cells anterior to the ablated region migrated normally. The black dotted lines indicate the anterior boundary of the uncaged cells on the non-ablated side.

(bracketed region in Fig. 5F). The cells posterior to the ablated region moved to a more anterior position than the corresponding cells on the unablated side within 6 h of ablation (Figs. 5B, E, and H, $n = 7$) and were found in the gonadal region at stage 35 (data not shown). *sdf-1a*-expressing cells located anterior to the somatic gonadal precursors, however, did not contribute to the most posterior region of the *sdf-1a* expression domain following loss of somatic gonadal precursors (Figs. 5A, D, and G, $n = 11$).

We next investigated if the lateral plate mesoderm, which included the posterior-most regions of the *sdf-1a* expression domain, exhibited prepatterning at the 6 somite stage. Several genes, such as *wt1*, *gata2*, *lim1*, and *sdf-1a*, known to be expressed in lateral cells in other vertebrates (Pelletier et al., 1991a,b; Detrich et al., 1995; Toyama and Dawid, 1997; Gering et al., 1998; Serluca and Fishman, 2001), clearly exhibited a demarcated expression pattern at the 6 somite stage as seen by whole mount in situ hybridization (Supplementary Fig. 4). These results indicated that the lateral plate mesoderm was prepatterned by the 6 somite stage.

The properties of the organ field are characterized by their ability to regulate the competence of that tissue before the organogenesis proceeds (Huxley and De Beer, 1934; DeRobertis et al., 1991). The ablation experiments, cell tracing experiments, and gene expression analyses all indicated that the posterior-most region of the *sdf-1a* expression domain at the 6 somite stage (stage 21) constitutes a gonadal field and had the ability to redirect posteriorly located cells, which are not prepatterned by *sdf-1a* expression, to follow the prepatterning and undergo a somatic gonadal fate.

Two distinct cell populations are spatially organized by the exclusive expression of ftz-f1 or sox9b before formation of a single gonadal primordium

At stage 30, *sdf-1a* expression was observed in both the somatic cells surrounding the PGCs and the medial somatic cells beneath the nephric ducts (Fig. 2E). We observed that *ftz-f1* expression at stage 30 was limited to *sdf-1a*-positive cells surrounding the PGCs; expression was not observed in the more medially positioned *sdf-1a*-expressing cells beneath the nephric ducts (compare Figs. 1B with 2E). To confirm that these two *sdf-1a*-positive cell populations both contributed to the somatic gonadal mesoderm, we labeled cells in either the anterior or posterior subregion of the gonadal field and followed the fates of the populations (Figs. 6A and E, and Supplementary Table 1). We determined that cells in the anterior gonadal field at the 10–11 somite stage (stage 22–23) positioned medially by stage 30 (Fig. 6B), localizing to the regions corresponding in cross-section to the medial domain of *sdf-1a* expression beneath the nephric duct (Fig. 6C). Surprisingly, we found that these medial *sdf-1a*-expressing cells also expressed the medaka homologue of *sox9b*, which is essential for testicular formation in mammals (Cameron et al., 1996; Kent et al., 1996; Morais da Silva et al., 1996; Bishop et al., 2000; Kluver et al., 2005; Nakamoto et al.,

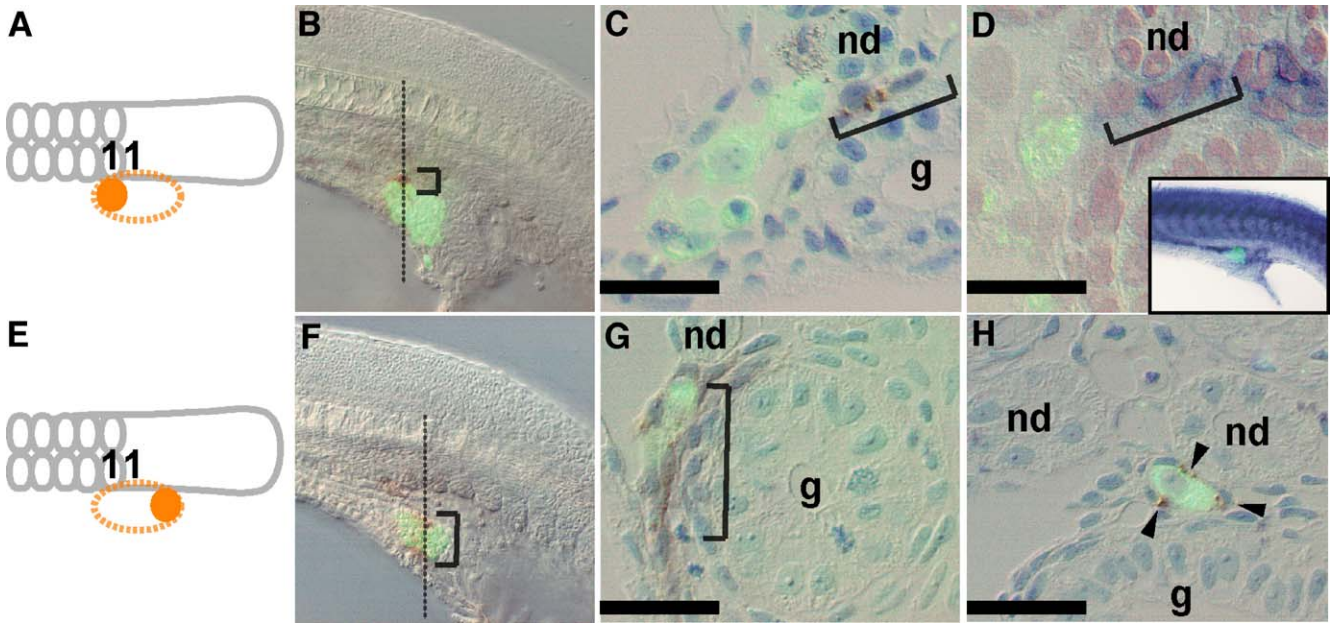

Fig. 6. Cells in the gonadal field are spatially organized into two populations of somatic gonadal precursors by stage 30. (A and E) Schematic representations indicating the positions of uncaged cells (brown circles) in the gonadal field (brown dotted circles) at the 10–11 somite stage (stage 22–23). (B and F) Lateral views of embryos at stage 30. The brackets indicate the locations of the uncaged cell progeny. (C and G) Cross-sections at the levels of the black lines shown in panels B and F, respectively. Labeling of cells in the anterior region (a brown circle) of the gonadal field (a brown dotted circle) at the 10–11 somite stage (stage 22–23) (A) revealed that their progeny (brown staining) contributed to the medial cells observed beneath the nephric ducts at stage 30 (B and C). Progeny (brown staining) of cells labeled in the posterior region (a brown circle) (E) contributed to cells surrounding the PGCs (green fluorescence) at stage 30 (F and G). (D) PGCs, detected by green fluorescence, are shown with *sox9b* expression (blue) at stage 30. Cells arising from the anterior portion of the gonadal field moved to the medial region, as indicated by a bracket within the region expressing *sox9b* at stage 30. The inset displays the expression of *sox9b*, as detected by whole mount in situ hybridization at stage 30 (lateral view). (H) The arrowheads indicate cells near the germ cells in the gonad at stage 35. These cells are descendants of the cells uncaged in the anterior half of the gonadal field (A). Descendants of the posterior half of the gonadal field also contribute to cells of the gonadal region at stage 35 (data not shown). (nd), nephric duct. (g), hindgut. Scale bar, 20 μm.

2005) (Fig. 6D). In contrast, at stage 30, cells situated in the posterior gonadal field (Fig. 6E) gave rise to the PGC-surrounding cells (Figs. 6F and G) that expressed both *sdf-1a* and *ftz-f1*, but not *sox9b* (Fig. 6D). Furthermore, cell labeling experiments indicated that both the anterior and posterior populations within the gonadal field contributed to the somatic gonadal mesoderm in the gonadal primordium at stage 35 (Fig. 6H and data not shown). These data clearly demonstrate that two different gonadal precursor lineages with distinct gene expression patterns are present before the onset of gonadogenesis. These populations became spatially organized into two populations along the anterior–posterior axis as early as the 10–11 somite stage (stages 22–23).

Discussion

The somatic precursors of more anteriorly positioned organs, such as the heart and kidney, have previously been characterized in non-amniotes (Fishman and Chien, 1997; Drummond, 2002). The development of somatic gonadal precursors, however, has largely been uncharacterized, perhaps due to the extreme ventral and posterior position of the gonad and the formation at a late developmental stage. Instead, attention has primarily been focused on sex differentiation following formation of the gonadal primordia (Brennan and Capel, 2004).

Prior to gonadal primordium formation, we fluorescently marked cells in medaka embryos and followed their movement and fates. At the 6 somite stage (stage 21), somatic gonadal precursors located in the most posterior subregion of the lateral plate mesoderm expressed *sdf-1a*, a chemoattractant for PGCs (Fig. 7A). During early somitogenesis, these bilateral precursor cells migrated medially and anteriorly to the levels of the eleventh and thirteenth somites. *sdf-1a* expression persisted in the precursors, which is consistent in position with the region to which *sdf-1a* expression becomes restricted. By the 13 somite stage (stage 23), somatic gonadal precursors organized into two populations along the anterior–posterior axis (Fig. 7B). Fate mapping studies demonstrated that the anterior subpopulation of somatic gonadal precursors distributed to the medial part of the lateral plate mesoderm beneath the nephric ducts at stage 30; in contrast, the more posterior subpopulation contributed to the more ventrolateral cells, which contacts and surrounds PGCs (Fig. 7C). Afterwards, the populations of somatic gonadal precursors located at the bilateral areas of the developing hindgut move medially (Fig. 7D), meeting at the prospective gonadal region on the dorsal side of the hindgut. Here, they form a clump of cells that comprise the single gonadal primordium (Figs. 1D and 6H). Expression analysis indicated that *sdf-1a* expression persisted in the gonadal precursors until their incorporation into the gonadal primordium.

Temporal properties of somatic gonadal precursors

Our results demonstrate that the lateral plate mesoderm was already prepatterned by early somitogenesis; recruitment of

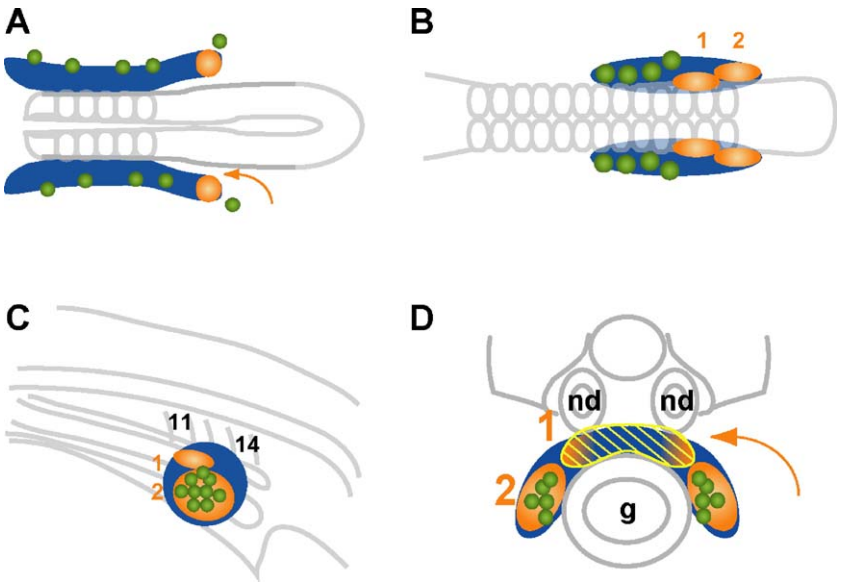

Fig. 7. Schematic representation of somatic gonadal precursor development. (A–C) Anterior is to the left. Dorsal views of embryos at the 6 (A) and 13 (B) somite stage (stage 21 and stage 23, respectively). Lateral view of an embryo (C) and a transverse section (D) at stage 30. Precursors of the somatic gonadal mesoderm (brown) are found at the most posterior portion of the *sdf-1a* expression domain (blue) (A) and move by convergent movement. During this movement, *sdf-1a* expression is lost in the anterior lateral plate mesoderm; the somatic gonadal precursors then become organized into two populations [at least by the 10–11 somite stage (stage 22–23)]. In accordance with the posterior restriction of *sdf-1a* expression, PGCs (green) become confined to the posterior portion of the *sdf-1a* expression domain (B), finally becoming surrounded by cells from population 2 (C). Specification of the somatic gonadal mesoderm occurs between the stages represented in panels B and C. The two populations are initially found at the levels of the eleventh to thirteenth somites then move medially to the prospective gonadal region on the dorsal side of the hindgut (D). After meeting together from both sides, a single gonadal primordium is formed (Fig. 1D), from which two bilateral gonads are derived during organogenesis (Hamaguchi, 1982; Kanamori et al., 1985). Population 1 cells express both *sdf-1a* (blue) and *sox9b* (yellow shadows), while population 2 cells express both *ftz-f1* and *sdf-1a* at stage 30.

more posteriorly locating cells that were not previously prepatterned as somatic gonadal precursors can compensate for the removal of somatic gonadal precursors. This result suggests that the lineage of cells in the posterior part of the *sdf-1a* expression domain was not yet specified as somatic gonadal precursors; instead, these cells were situated in a gonadal field capable of instructing the cells to adopt a somatic gonadal mesoderm fate (Fig. 7A). Together with the fact that PGCs migrate towards posterior end of *sdf-1a* expression domain, this result implies that the gonadal field can be defined as the region coordinating PGC migration by persistent *sdf-1a* expression with the development of gonadal precursors.

Ablation experiments at later stages suggested that by stage 26 the somatic gonadal precursors in this field have been specified as somatic gonadal mesoderm, as demonstrated by the loss of expression of both *ftz-f1* and *amh* at stage 35. By this stage, gonadal precursors are positioned bilaterally adjacent to the axial structures at the levels of the eleventh to thirteenth somites, consistent with the position of the gonad along the anterior–posterior axis (Figs. 7B and C). Previous work has demonstrated that the axial structures, including the endoderm and notochord, play a critical role in heart development (Schultheiss et al., 1995; Goldstein and Fishman, 1998). Juxtaposition of the precursor cells and the axial structures, as well as the timing of cell lineage commitment, may suggest that signals from the axial structures are involved in specification of the gonadal mesoderm.

Two different populations of somatic gonadal precursors

Our marker gene expression analyses demonstrated the presence of two populations of *sdf-1a*-expressing cells at stage 30 (brown regions 1 and 2 in Figs. 7C and D). One population (brown region 2) surrounds the PGCs and expresses both *ftz-f1* and *sdf-1a*. The mammalian homologue of *ftz-f1*, *Ad4BP/SF1*, functions in the establishment and maintenance of the gonad (Luo et al., 1994; Sadovsky et al., 1995). Our lineage analyses indicated that descendants of this population contributed to the somatic gonadal mesoderm. These data suggest that cells expressing *ftz-f1* and *sdf-1a* are already established as gonadal mesoderm before reaching the gonadal area.

The other *sdf-1a*-expressing population (brown region 1), which expressed *sox9b* (yellow shadow in Fig. 7D), consists of cells just anterior and medial to the *ftz-f1*/*sdf-1a*-positive region (brown region 2). Although we could not detect *ftz-f1* expression in these cells at stage 30, our cell tracing experiments clearly demonstrate that this population of cells is also observed in the gonadal mesoderm at later stages. These results indicate that the cells, which are *sdf-1a/sox9b*-positive and *ftz-f1*-negative at stage 30, also constitute part of the gonadal mesoderm.

These two populations of somatic gonadal precursors began to be spatially organized at around the 10–11 somite stage (stage 22–23). Although the lateral cells moved medially to underlie the axial structures, which made labeling by uncaging technically difficult, cell labeling experiments at the 10–11

somite stage (stage 22–23) demonstrate that the *ftz-f1*/*sdf-1a*-expressing cells at stage 30 arise from the posterior half of the gonadal field whereas the *ftz-f1*-negative/*sdf-1a*/*sox9b*-positive cells are derived from the more anterior region of the field (Supplementary Table 1). This indicates that the somatic gonadal precursors are spatially organized before they became irreplaceable by the surrounding cells at stage 26.

Our data demonstrate that PGCs are attracted to the gonadal field in which somatic gonadal precursors arise. Somatic gonadal precursors become established before formation of the primordium. Furthermore, we demonstrated that distinct cell populations marked by differential gene expression contribute to the gonadal mesoderm. These results provide new insight into the development of somatic gonadal precursors and the mechanisms underlying sex differentiation.

Acknowledgments

We are grateful to Dr. Sasado for technical advice on the preparation of histological samples, Drs. Kobayashi, Sato, and Hayashi for technical advice about the TSA Biotin System, Dr. Morohashi for help with confocal microscopy, Dr. Takeda for providing us with the medaka *nanos* cDNA, Drs. Araki and Inohaya for providing the medaka *lim1* cDNA, and Drs. Miyawaki and Nagai for providing information about PA-Venus. We also thank Ms. Ichikawa and Kuboshita for fish maintenance. This work was supported by Grants-in-Aid for Scientific Research (15310133, 17370083, 17012027) and by the JSPS (Japan Society for the Promotion of Science) fellows of Ministry of Education, Culture, Sports, Science and Technology of Japan.

Appendix A. Supplementary data

Supplementary data associated with this article can be found, in the online version, at doi:10.1016/j.ydbio.2006.03.052.

References

Ara, T., Nakamura, Y., Egawa, T., Sugiyama, T., Abe, K., Kishimoto, T., Matsui, Y., Nagasawa, T., 2003. Impaired colonization of the gonads by primordial germ cells in mice lacking a chemokine, stromal cell derived factor-1 (SDF-1). Proc. Natl. Acad. Sci. U. S. A. 100, 5319–5323.

Bishop, C.E., Whitworth, D.J., Qin, Y., Agoulnik, A.I., Agoulnik, I.U., Harrison, W.R., Behringer, R.R., Overbeek, P.A., 2000. A transgenic insertion upstream of sox9 is associated with dominant XX sex reversal in the mouse. Nat. Genet. 26, 490–494.

Brennan, J., Capel, B., 2004. One tissue, two fates: molecular genetic events that underlie testis versus ovary development. Nat. Rev., Genet. 5, 509–521.

Cameron, F.J., Hageman, R.M., Cooke-Yarborough, C., Kwok, C., Goodwin, L.L., Sillence, D.O., Sinclair, A.H., 1996. A novel germ line mutation in SOX9 causes familial campomelic dysplasia and sex reversal. Hum. Mol. Genet. 5, 1625–1630.

Capel, B., Albrecht, K.H., Washburn, L.L., Eicher, E.M., 1999. Migration of mesonephric cells into the mammalian gonad depends on *Sry*. Mech. Dev. 84, 127–131.

DeRobertis, E.M., Morita, E.A., Cho, K.W.Y., 1991. Gradient fields and homeobox genes. Development 112, 669–678.

Detrich III, H.W., Kieran, M.W., Chan, F.Y., Barone, L.M., Yee, K., Rundstadler, J.A., Pratt, S., Ransom, D., Zon, L.I., 1995. Intraembryonic hematopoietic cell migration during vertebrate development. Proc. Natl. Acad. Sci. U. S. A. 92, 10713–10717.

Doitsidou, M., Reichman-Fried, M., Stebler, J., Koprunner, M., Dorries, J., Meyer, D., Esguerra, C.V., Leung, T., Raz, E., 2002. Guidance of primordial germ cell migration by the chemokine SDF-1. Cell 111, 647–659.

Drummond, I., 2002. The pronephros. Results. Prob. Cell Differ. 40, 322–345.

Fishman, M.C., Chien, K.R., 1997. Fashioning the vertebrate heart: earliest embryonic decisions. Development 124, 2099–2117.

Gering, M., Rodaway, A.R., Gottgens, B., Patient, R.K., Green, A.R., 1998. The SCL gene specifies haemangioblast development from early mesoderm. EMBO J. 17, 4029–4045.

Goldstein, A.M., Fishman, M.C., 1998. Notochord regulates cardiac lineage in zebrafish embryos. Dev. Biol. 201, 247–252.

Hamaguchi, S., 1982. A light microscopic and electron microscopic study on the migration of primordial germ cells in the teleost, *Oryzias latipes*. Cell Tissue Res. 227, 139–151.

Hatano, O., Takakusu, A., Nomura, M., Morohashi, K., 1996. Identical origin of adrenal cortex and gonad revealed by expression profiles of Ad4BP/SF-1. Genes Cells 1, 663–671.

Huxley, J., De Beer, G., 1934. The Elements of Experimental Embryology. The Univ. Press, Cambridge.

Iwamatsu, T., 1994. Stages of normal development in the medaka *Oryzias latipes*. Zool. Sci. 11, 825–839.

Iwamatsu, T., 2004. Stages of normal development in the medaka, *Oryzias latipes*. Mech. Dev. 121, 605–618.

Kanamori, A., Nagahama, Y., Egami, N., 1985. Development of the tissue architecture in the gonads of the medaka *Oryzias latipes*. Zool. Sci. 2, 695–706.

Keller, R., Davidson, L., Edlund, A., Elul, T., Ezin, M., Shook, D., Skoglund, P., 2000. Mechanisms of convergence and extension by cell intercalation. Philos. Trans. R. Soc. London, Ser. B Biol. Sci. 355, 897–922.

Kent, J., Wheatley, S.C., Andrews, J.E., Sinclair, A.H., Koopman, P., 1996. A male-specific role for SOX9 in vertebrate sex determination. Development 122, 2813–2822.

Kluver, N., Kondo, M., Herpin, A., Mitani, H., Schartl, M., 2005. Divergent expression patterns of Sox9 duplicates in teleosts indicate a lineage specific subfunctionalization. Dev. Genes Evol. 215, 297–305.

Knaut, H., Werz, C., Geisler, R., Nüsslein-Volhard, C., 2003. A zebrafish homologue of the chemokine receptor Cxcr4 is a germ cell guidance receptor. Nature 421, 279–282.

Kosman, D., Mizutani, C.M., Lemons, D., Cox, W.G., McGinnis, W., Bier, E., 2004. Multiplex detection of RNA expression in *Drosophila* embryos. Science 305, 846.

Kurokawa, H., Aoki, Y., Nakamura, S., Ebe, Y., Kobayashi, D., Tanaka, M., 2006. Time-lapse analysis reveals different modes of primordial germ cell migration in medaka (*Oryzias latipes*). Dev. Growth Differ. 48, 209–221.

Luo, X., Ikeda, Y., Parker, K.L., 1994. A cell specific nuclear receptor is essential for adrenal and gonadal development and sexual differentiation. Cell 77, 481–490.

Martineau, J., Nordqvist, K., Tilmann, C., Lovell-Badge, R., Capel, B., 1997. Male-specific cell migration into the developing gonad. Curr. Biol. 7, 958–968.

Molyneaux, K.A., Zinszner, H., Kunwar, P.S., Schaible, K., Stebler, J., Sunshine, M.J., O'Brien, W., Raz, E., Littman, D., Wylie, C., Lehmann, R., 2003. The chemokine SDF1/CXCL12 and its receptor CXCR4 regulate mouse germ cell migration and survival. Development 130, 4279–4286.

Morais da Silva, S., Hacker, A., Harley, V., Goodfellow, P., Swain, A., Lovell-Badge, R., 1996. Sox9 expression during gonadal development implies a conserved role for the gene in testis differentiation in mammals and birds. Nat. Genet. 14, 62–68.

Morinaga, C., Tomonaga, T., Sasado, T., Suwa, H., Niwa, K., Yasuoka, A., Henrich, T., Watanabe, T., Deguchi, T., Yoda, H., Hirose, Y., Iwanami, N., Kunimatsu, S., Okamoto, Y., Yamanaka, T., Shinomiya, A., Tanaka, M., Kondoh, H., Furutani-Seiki, M., 2004. Mutations affecting gonadal development in medaka, *Oryzias latipes*. Mech. Dev. 121, 829–839.

Münsterberg, A., Lovell-Badge, R., 1991. Expression of the mouse anti-müllerian hormone gene suggests a role in both male and female sexual differentiation. Development 113, 613–624.

Nagai, T., Ibata, K., Park, E.S., Kubota, M., Mikoshiba, K., Miyawaki, A., 2002.

A variant of yellow fluorescent protein with fast and efficient maturation for cell-biological applications. Nat. Biotechnol. 20, 87–90.

Nakamoto, M., Suzuki, A., Matsuda, M., Nagahama, Y., Shibata, N., 2005. Testicular type Sox9 is not involved in sex determination but might be in the development of testicular structures in the medaka, *Oryzias latipes*. Biochem. Biophys. Res. Commun. 333, 729–736.

Oguri, M., 1961. Histomorphology on the kidney and adrenal gland of medaka, *Oryzias latipes*. Bull. Jpn. Soc. Sci. Fish. 27, 1058–1062.

Oliver, G., Loosli, F., Koster, R., Wittbrodt, J., Gruss, P., 1996. Ectopic lens induction in fish in response to the murine homeobox gene Six3. Mech. Dev. 60, 233–239.

Patterson, G.H., Lippincott-Schwartz, J., 2002. A photoactivatable GFP for selective photolabeling of proteins and cells. Science 297, 1873–1877.

Pelletier, J., Schalling, M., Buckler, A.J., Rogers, A., Haber, D.A., Housman, D., 1991a. Expression of the Wilms' tumor gene WT1 in the murine urogenital system. Genes Dev. 5, 1345–1356.

Pelletier, J., Bruening, W., Li, F.P., Haber, D.A., Glaser, T., Housman, D.E., 1991b. WT1 mutations contribute to abnormal genital system development and hereditary Wilms' tumour. Nature 353, 431–434.

Rodemer, E.S., Ihmer, A., Wartenberg, H., 1986. Gonadal development of the chick embryo following microsurgically caused agenesis of the mesonephros and using interspecific quail–chick chimaeras. J. Embryol. Exp. Morphol. 98, 269–285.

Ronshaugen, M., Levine, M., 2004. Visualization of trans-homolog enhancer–promoter interactions at the Abd-B Hox locus in the *Drosophila* embryo. Dev. Cell 7, 925–932.

Sadovsky, Y., Crawford, P.A., Woodson, K.G., Polish, J.A., Clements, M.A., Tourtellotte, L.M., Simburger, K., Milbrandt, J., 1995. Mice deficient in the orphan receptor steroidogenic factor 1 lack adrenal glands and gonads but express P450 side-chain-cleavage enzyme in the placenta and have normal embryonic serum levels of corticosteroids. Proc. Natl. Acad. Sci. U. S. A. 92, 10939–10943.

Schultheiss, T.M., Xydas, S., Lassar, A.B., 1995. Induction of avian cardiac myogenesis by anterior endoderm. Development 121, 4203–4214.

Serbedzija, G.N., Chen, J.N., Fishman, M.C., 1998. Regulation in the heart field of zebrafish. Development 125, 1095–1101.

Serluca, F.C., Fishman, M.C., 2001. Pre-pattern in the pronephric kidney field of zebrafish. Development 128, 2233–2241.

Shinomiya, A., Tanaka, M., Kobayashi, T., Nagahama, Y., Hamaguchi, S., 2000. The vasa-like gene, olvas, identifies the migration path of primordial germ cells during embryonic body formation stage in the medaka. Dev. Growth Differ. 42, 317–326.

Stebler, J., Spieler, D., Slanchev, K., Molyneaux, K.A., Richter, U., Cojocaru, V., Tarabykin, V., Wylie, C., Kessel, M., Raz, E., 2004. Primordial germ cell migration in the chick and mouse embryo: the role of the chemokine SDF-1/CXCL12. Dev. Biol. 272, 351–361.

Tanaka, M., Kinoshita, M., Kobayashi, D., Nagahama, Y., 2001. Establishment of medaka (*Oryzias latipes*) transgenic lines with the expression of green fluorescent protein fluorescence exclusively in germ cells: a useful model to monitor germ cells in a live vertebrate. Proc. Natl. Acad. Sci. U. S. A. 98, 2544–2549.

Thisse, C., Zon, L.I., 2002. Organogenesis—Heart and blood formation from the zebrafish point of view. Science 295, 457–462.

Tilmann, C., Capel, B., 1999. Mesonephric cell migration induces testis cord formation and Sertoli cell differentiation in the mammalian gonad. Development 126, 2883–2890.

Toyama, R., Dawid, I.B., 1997. *lim6*, a novel LIM homeobox gene in the zebrafish: comparison of its expression pattern with *lim1*. Dev. Dyn. 209, 406–417.

Watanabe, M., Tanaka, M., Kobayashi, D., Yoshiura, Y., Oba, Y., Nagahama, Y., 1999. Medaka (*Oryzias latipes*) FTZ-F1 potentially regulates the transcription of P-450 aromatase in ovarian follicles: cDNA cloning and functional characterization. Mol. Cell. Endocrinol. 149, 221–228.

Yasuoka, A., Hirose, Y., Yoda, H., Aihara, Y., Suwa, H., Niwa, K., Sasado, T., Morinaga, C., Deguchi, T., Henrich, T., Iwanami, N., Kunimatsu, S., Abe, K., Kondoh, H., Furutani-Seiki, M., 2004. Mutations affecting the formation of posterior lateral line system in medaka, *Oryzias latipes*. Mech. Dev. 121, 729–738.